

Harvesting energy from acoustic vibrations of conventional and ultrasonic whistles

Rebecca Hattery^{1a} and Onur Bilgen^{*1,2}

¹Department of Mechanical and Aerospace Engineering, Old Dominion University, Norfolk, Virginia, 23529, USA

²Department of Mechanical & Aerospace Engineering Rutgers, The State University of New Jersey
98 Brett Road, Piscataway, NJ 08854, USA

(Received September 19, 2016, Revised April 19, 2017, Accepted April 20, 2017)

Abstract. This paper experimentally investigates the feasibility of harvesting vibration energy from whistles using piezoelectric materials. The end goal of this research is to generate sufficient power from the whistle to power a small radio transmitter to relay a basic signal – for example, a distress call. First, the paper discusses the current literature in energy harvesting from acoustic resonance. Next, the concept of an active whistle is presented. Next, results from energy harvesting experiments conducted on conventional and ultrasonic whistles undergoing human-actuation and actuation by a pressure-regulated air supply are presented. The maximum power density of the conventional whistle actuated by a human at 100 dB sound pressure level is $98.1 \mu\text{W}/\text{cm}^3$.

Keywords: piezoelectric materials; acoustics; vibration energy harvesting; whistle

1. Introduction

Manual signaling devices, such as whistles, operate in a variety of situations without any electrical requirements; however, their transmission range may be severely limited compared to radio-frequency (RF) based devices. Emergency signaling devices can be automatic, which require no human effort to function, or semi-automatic or manual, which require some human effort to operate. Typically, modern signaling devices, such as emergency locator transponders, cellular phones, and two-way radios, require an electrical supply to function. Human interaction with manual signaling devices can be used to generate vibration energy; this mechanical energy may be converted to useful electrical energy. Vibration energy harvesters capture ambient vibrations and transduce the mechanical energy into electrical energy. Comprehensive reviews of energy harvesting using piezoelectric materials are provided by Sodano (2004), Anton (2007), Cook-Chennault *et al.* (2008), and Priya and Inman (2009). This paper proposes a human powered vibration energy harvester that uses acoustic vibrations of a whistle to generate power to transmit a signal using a radio transmitter. The application of human-generated power to the field of piezoelectric energy harvesting is significant. The successful integration of a commonly used device, such as a whistle, with an energy-generating substance, such as piezoelectric material, proves the concept of using piezoelectric energy harvesting

to augment the signaling abilities of the whistle. In this context, the following sections will present a detailed literature survey on harvesting energy from acoustic resonance.

Acoustic resonance is a wave phenomenon that is a function of the fundamental vibration frequency of an instrument or one of the fundamental harmonics (Bueche 1969). Acoustic resonators exhibit both a mechanical and an auditory resonant behavior. Acoustic resonance can occur within any hollow chamber where nodes and antinodes form due to changes in air pressure (Bueche 1969). Two common acoustic resonators are pipe resonators and Helmholtz resonators. Pipe resonators are hollow pipes with either open or closed ends which amplify sound based on the relationship between the resonant frequency and the length of the pipe. A Helmholtz resonator is a hollow container with an open neck; this resonator responds with both an audible tone and mechanical vibrations if a pressure differential is applied across the open neck. The resonance response can be used in energy harvesting applications. Sherrit (2008) used an equivalent circuit model to review and compare different methods of harvesting energy from acoustic resonance. Pillai and Deenadayalan (2014) reviewed acoustic and thermoacoustic energy harvesting techniques. Table 1 summarizes research in vibration energy harvesting with acoustic resonators relevant to this paper. Acoustic input level is measured in sound pressure level (SPL) and quantified in decibel (dB).

Matsuda *et al.* (2013) developed a Helmholtz resonator energy harvester with a variable polarity circular piezoelectric material membrane. A sound-focusing acoustic cone increased the power harvested from 1.7×10^{-13} W to 6.8×10^{-13} W at 110 dB SPL. Horowitz (2005, 2006) proposed a MEMS acoustic energy harvester which was a Helmholtz resonator with a compliant diaphragm. The

*Corresponding author, Assistant Professor

E-mail: obilgen@rutgers.edu

^aM.S.

E-mail: rebecca.s.hattery@gmail.com

Table 1 Literature with acoustic resonators as a source of vibration energy

Year	Authors	Notes / Significance	Type	Power
2003	Matsuda <i>et al.</i>	PZT based – an early example	Helmholtz	0.68 pW 110 dB
2005	Horowitz <i>et al.</i>	MEMS device	Helmholtz	0.34 $\mu\text{W}/\text{cm}^3$
2006	Horowitz <i>et al.</i>	MEMS device	Helmholtz	0.34 $\mu\text{W}/\text{cm}^3$
2008	Liu <i>et al.</i>	highest power output in this review	Helmholtz	30 mW 160 dB
2009	Kim <i>et al.</i>	electromagnetic transduction from direct airflow	Helmholtz	15 mV _{pp}
2009	Wu <i>et al.</i>	resonant cavity	Sonic Crystal	40 nW
2010	Wang <i>et al.</i>	piezoelectric curved beams	Sonic Crystal	37 nW
2012	Bibo and Daqaq	harmonica-type	Pipe	55 μW
2012	Li <i>et al.</i>	quarter wavelength straight-tube resonator	Pipe	55 $\mu\text{W}/\text{cm}^2$ 110 dB
2013	Khan and Izhar	proposed for wireless sensor nodes	Helmholtz	191 $\mu\text{W}/\text{cm}^3$ 120 dB
2013	Moriyama <i>et al.</i>	piezoelectric element	Pipe	
2013	Li <i>et al.</i>	PZT plates in a straight tube resonator	Pipe	1.37 $\mu\text{W}/\text{cm}^3$ 100 dB
2014	Sun <i>et al.</i>	using vortex shedding effect	Helmholtz	95.5 $\mu\text{W}/\text{cm}^3$
2014	Yang <i>et al.</i>	broadband - dual piezoelectric cantilever beams	Helmholtz	360 nW/cm ³ 120 dB
2015	Aladwani <i>et al.</i>	two-dimensional coupled acoustic-structure system with a dynamic magnifier	Helmholtz	

maximum power density was $0.34 \mu\text{W}/\text{cm}^2$. Liu *et al.* (2008) compared vibration energy harvested using Helmholtz resonators with a direct charging circuit and a flyback converter circuit; the flyback circuit converted 260% more energy than a conventional circuit. The maximum power harvested was 30 mW at 160 dB SPL. Sun *et al.* (2014) used a Helmholtz resonator with a pressurized fluid and inlet bluff bodies to generate high frequency vibrations. The resonator with the bluff body had a $95.5 \mu\text{W}/\text{cm}^3$ power density at 4.2 psi inlet pressure. Yang *et al.* (2014) proposed a Helmholtz resonator with dual piezocomposite cantilever beams mounted on the top surface. The dual beam system was proposed to expand the frequency range available for harvesting energy. The maximum power density was $0.360 \mu\text{W}/\text{cm}^3$ at 100 dB SPL. Kim *et al.* (2009) proposed an electromagnetic acoustic energy harvester in which the vibrations in the Helmholtz resonator base displaced a small magnet through a wire coil. The maximum voltage generated was 15 mV_{pp}. Khan (2013) demonstrated a Helmholtz resonator with a flexible membrane driving an electromagnetic generator. The maximum power density was $191.4 \mu\text{W}/\text{cm}^3$ at 120 dB SPL.

Li (2012) proposed a quarter-wavelength straight-tube

resonator with several piezocomposite beams along the tube centerline to harvest energy. The maximum power density was $0.055 \text{mW}/\text{cm}^2$ at 110 dB SPL. Li (2013) researched power generation using tube resonators with multiple PZT plates. The maximum power density was $1.367 \mu\text{W}/\text{cm}^3$ at 100 dB SPL.

Wu (2009) and Wang (2010) proposed resonant cavities in sonic crystals as energy harvesting vibration sources. The voltage generated by a piezocomposite beam in the cavity was 25 times higher than the voltage generated by a beam activated outside the cavity. The maximum power generated was 40 nW. Bibo *et al.* (2012) proposed a harmonica-like structure in which a piezocomposite reed transforms energy from moving air into electrical energy via acoustic vibrations. The maximum power generated was $55 \mu\text{W}$. Moriyama *et al.* (2013) modeled and developed an energy harvester using vibroacoustic coupling between a cylinder and its flat end-plates; the vibration energy was harvested via piezoelectric disks mounted on the flat end-plates. Aladwani *et al.* (2015) presented a finite element model of coupled acoustic-structure vibration energy harvester with a dynamic magnifier. The base structure was connected with a spring to a simply-supported piezocomposite beam energy harvester. The base natural frequency was matched to the

beam's first natural frequency to increase the harvested energy.

Starner and Paradiso (2004) provide an overview of human mechanisms to generate power. The mechanisms discussed were metabolic processes, thermal radiation, respiration, and motion such as walking or gesturing. Paradiso and Starner (2005) also reviewed human-supplied energy scavenging systems. The paper focused on the insertion of piezoelectric vibration energy harvesters into shoes to capture vibration energy from walking. Karami and Inman (2012) proposed a pacemaker which was charged using piezoelectric materials activated by vibrations from heartbeats. Sue and Tsai (2012) provided an overview of a microelectromechanical system (MEMS) based energy harvester which relied on human-generated power to supply to implanted medical devices. The harvesters reviewed are both implanted harvesters and wearable harvesters.

The objective of this paper is to demonstrate the feasibility of the use of acoustic resonance of whistles as an energy source. In this context, the mechanical and electrical behavior of conventional and ultrasonic whistles mounted with a piezoelectric disk is examined. Based on the literature survey presented above, there are no known examples of whistles used as a source of vibration energy in the literature; hence, the concept presented on this paper is unique to the best knowledge of the authors.

The paper is organized as follows: First, the concept of whistle-acoustic-energy-harvester is presented. The harvesting behavior of different types of whistles, and the response to human-actuation and actuation with a pressure-regulated air supply are examined. Conclusions are presented.

2. The concept of an active whistle

This paper proposes using vibration energy from a whistle to generate electricity for powering a secondary electronic signaling device. For example, the harvested energy can be used to power a small radio transmitter to emit an electronic locator signal for emergencies. The RF signal augments the acoustic signal of the whistle to provide location information to emergency responders. The proposed concept is illustrated in Fig. 1.

Although the harvested energy can be used to power an RF-based signaling device such as an RF transmitter, the system-level analysis of the concept proposed in Fig. 1 is outside of the scope of this paper. The research in this paper focuses on the problem of harvesting energy from whistles, more specifically, conventional and ultrasonic whistles. Piezoceramic disks can be mounted on the flat sidewall of a conventional whistle or on the flat end of an ultrasonic whistle to capture the vibration energy. In the case of the conventional whistle, the placement of the piezoelectric transducer is based on an understanding of the free transverse vibration of clamped circular plates. In the case of the ultrasonic whistle, axial vibration of the whistle body, which is a bar-like structure, is of interest.

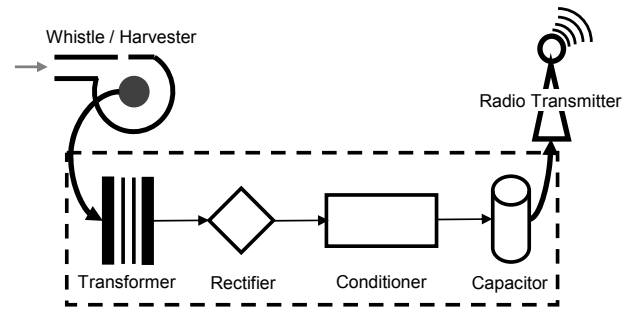


Fig. 1 The whistle-powered radio transmitter concept

3. Experimental prototypes

The pressure inside of the whistle chamber is a function of inlet flow and chamber geometry, and it is logical to assume that the pressure distribution is non-uniform (spatially) and dynamic (temporally.) For the conventional whistle, it was previously noted that the out-of-plane displacement of the chamber wall where the disk is attached, and consequently the strain induced on the disk, is of interest for power generation. Since the sidewall has significant bending rigidity and it acts like a plate, non-uniform pressure will not significantly affect the operating deflection shape. Consequently, the first axisymmetric mode is likely to be dominant. For the ultrasonic whistle, the only flat surface is the end of the whistle; hence, the axial extension-compression of the whistle is relevant. This mode of vibration will axially extend and compress the PZT disk against the so-called end-mass.

For the types of structures considered in this paper, a basic understanding of the displacement and strain behavior is necessary to maximize induced strain and to avoid internal charge cancellation. Such cancellation occurs due to strain reversals in beam- and plate-like structures under certain types of boundary conditions. As the primary application considered here is a conventional whistle, a relevant structure is a fully clamped circular plate. For the ultrasonic whistle, the placement is mainly dictated by physical constraints rather than strain distribution. It should be noted that strain cancellation is not expected in axial vibrations of short bar-like (e.g., a disk) structures; hence, the choice of placement of the piezoelectric transducer on the ultrasonic whistle is considered obvious. In the following section, a brief background on the choice of piezoelectric transducer placement for the conventional whistle is presented. Next, the design of two experimental prototypes are shown and discussed.

3.1 Piezoelectric transducer placement

For the conventional whistle, the displacement and strain distributions of the flat side walls of the whistle are calculated using the classical plate theory (Szilard 1973). The classical plate theory assumes that the plate is elastic, homogeneous and isotropic, is thin relative to length and width, has small deflections relative to plate thickness, has deflections represented by the mid-surface, and the maximum mid-surface slope is small. Straight lines normal

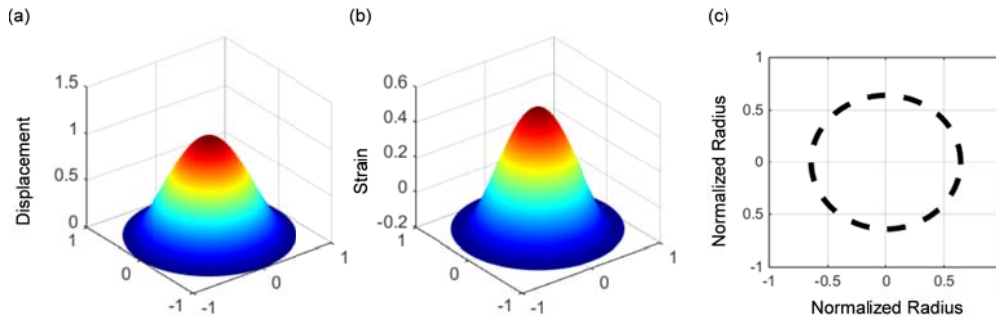


Fig. 2 The first axisymmetric mode of a fully clamped circular plate: (a) deflection mode shape, (b) strain mode shape, and (c) strain nodal circle

to the middle surface remain straight and normal under deflection, implying that transverse shear is neglected. Stresses normal to the plate mid-plane are assumed negligible. The plate is assumed flat prior to actuation. The displacement field is assumed to be in the following form (Reddy 1999)

$$\begin{aligned} u(x, y, z, t) &= u_0(x, y, t) - z \frac{\partial w_0}{\partial x}, \\ v(x, y, z, t) &= v_0(x, y, t) - z \frac{\partial w_0}{\partial y}, \\ w(x, y, z, t) &= w_0(x, y, t) \end{aligned} \quad (1)$$

where u , v , and w are the deformations along the x , y , and z coordinates, respectively. The thickness direction is represented by z , and time is represented by t . The subscript 0 indicates the midplane. The equation of motion for the axisymmetric response of a fully clamped circular plate is given by (Shames and Dym 1985)

$$D\nabla^4 w + \rho h \ddot{w} = q \quad (2)$$

where D is the plate bending stiffness, ∇^4 is the square of the Laplacian operator, ρ is the material density, h is the plate thickness, and q is the applied loading. The equation of motion can be solved for the free response using separation of variables. The expression for plate free-response is given by (Szilard 1973)

$$w(r, t) = \left(J_0(kr) + \frac{J_1(ka)}{I_1(ka)} I_0(kr) \right) \left(\frac{w_0}{1 + \frac{J_1(ka)}{I_1(ka)}} \cos(\omega t) \right), \quad (3)$$

where J_0 , I_0 , J_1 , and I_1 are Bessel functions, k is the modal coordinate, r is the radial position, a is the radius, and ω is the frequency of vibration. The first part of Eq. (3) is the zeroth-mode plate mode shape, which is the lowest-order axisymmetric plate mode response to initial conditions. The reader is referred to Leissa (1969) for a complete treatment of axisymmetric plate mode shapes. The plate radial strain is related to the plate displacement by (Reddy 1999)

$$\varepsilon_r = -z \frac{d^2 w}{dr^2}, \quad (4)$$

where ε_r is the radial strain. The strain is proportional to the vertical location within the plate; therefore, the strain nodes, or locations where the strain switches polarity, can be found from the second derivative of the mode shape

$$\begin{aligned} \frac{d^2 w}{dr^2} &= \frac{1}{2} (J_0(kr) - J_2(kr)) \\ &+ \frac{J_1(ka)}{2I_1(ka)} (I_0(kr) + I_2(kr)) \end{aligned} \quad (5)$$

The normalized displacement and strain response is shown in Fig. 2.

The first axisymmetric strain shape and the nodal circle are used to place the piezoceramic disk on the conventional whistle such that the piezoelectric disk will experience maximum strain and therefore generate maximum power. A series of experiments are conducted to validate the theoretical predictions of displacement and strain mode shapes – the reader is referred to Hattery (2015) for details.

3.2 Prototypes

Fig. 3 shows the two prototypes fabricated using two commercially available whistles. In both devices, a piezoceramic disk is bonded to the “best” flat surface available on the whistle using conductive epoxy. The conventional whistle is approximately 40 mm long and 19 mm wide, and has two flat sidewalls supported by a drum-like chamber (20 mm diameter and 17 mm height) as shown in Fig. 3(a). The sidewalls can be described as clamped circular disks and provide an excellent flat surface for the attachment of the piezoelectric disk. In contrast, the ultrasonic whistle is a 45 mm long slender tube with 8 mm outer diameter– the only flat surface is the closed end of the whistle as shown in Fig. 3(c). The acoustic chamber of this whistle is approximately 12 mm tall and has an inner diameter of 4 mm.

The properties of the piezoceramic disk transducers are presented in Table 2.

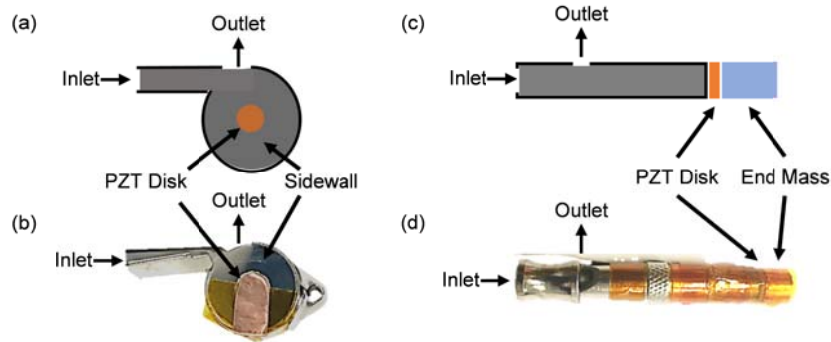


Fig. 3 Conventional whistle (a) illustration, and (b) picture. Ultrasonic whistle (c) illustration, and (d) picture. Dimensions in the illustrations are exaggerated to aid visibility

Table 2 Piezoceramic disk properties used in both prototypes (Piezo Systems 2015)

Property	Value	Units
Diameter	6.35	mm
Thickness	0.19	mm
Volume	0.024	cm ³
Density	7800	kg/m ³
Elastic Modulus (Y_3^E)	52	GPa
Elastic Modulus (Y_1^E)	66	GPa
d_{31}	-190	pC/N
d_{33}	390	pC/N
Capacitance	2.7	nF

The conventional whistle has resonant frequencies in the range of human hearing and has a large flat side surface similar to a clamped circular plate. The dominant mode of mechanical transduction utilized is the strain induced by bending of the circular side surface. Based on the strain analysis presented in the previous section, a small piezoelectric disk-type transducer is bonded to the center of the sidewall of the whistle chamber.

In the case of the ultrasonic whistle, the device has at least one audible resonant frequency, and has other resonant frequencies in the ultrasonic range that is audible by dogs. As the ultrasonic whistle is a relatively short bar-like structure, there are a limited number of options for the placement of the piezoelectric disk. A practical location is the end of the ultrasonic whistle and the disk is bonded to this location. A 0.20 gram proof-mass is bonded to the other surface of the piezoceramic disk on the ultrasonic whistle to add inertial resistance to acceleration (as it is done in an accelerometer.) In the case of the ultrasonic whistle, the dominant mode of mechanical transduction utilized is the strain induced by the axial load due to the inertia of the end mass.

4. Experimental demonstration

In this section, the experimental demonstration and results are presented, and the electrical responses of the two prototypes are compared. The electrical output of the piezoelectric disks in response to acoustic excitation is quantified by measuring the voltage output of the disks across a resistive shunt. In the experiments, the whistles are operated either by human-actuation or by pressure-regulated air. Fig. 4 shows the apparatus and an illustration of the experimental setup.

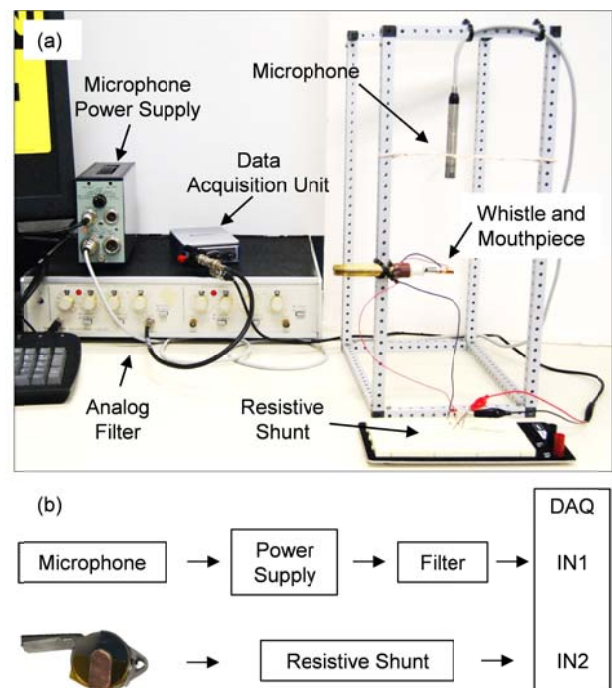


Fig. 4 Experimental (a) apparatus, and (b) signal flow for energy harvesting tests

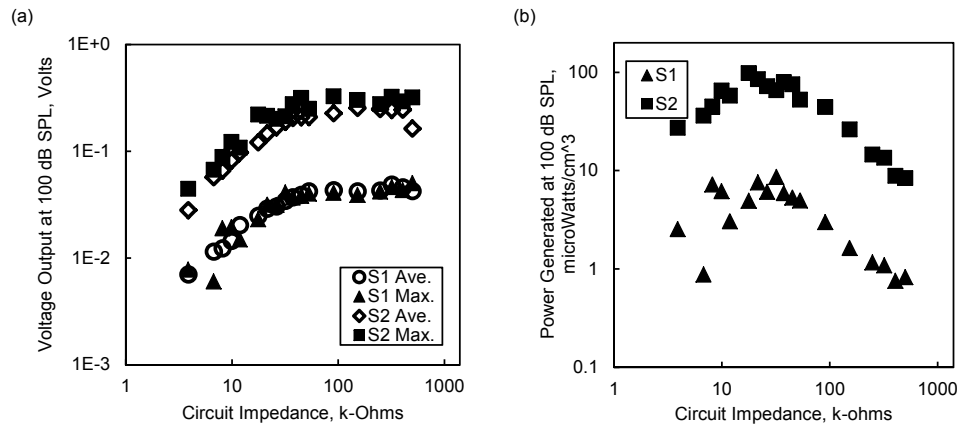


Fig. 5 Comparison of normalized voltage output and power density at resonance as a function of circuit impedance as generated by a conventional whistle undergoing average and maximum human-actuation

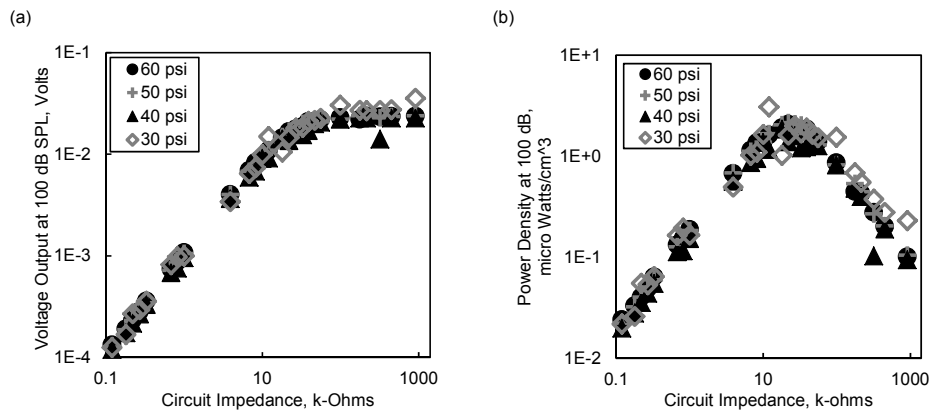


Fig. 6 Comparison of normalized voltage output and power density of the conventional as a function of circuit impedance in response to actuation using a pressure-regulated air supply at 30, 40, 50, and 60 psi

The acoustic response is measured using a B&K type 4190 microphone. The microphone is placed 10 cm from the whistle airflow outlet in accordance with the manufacturer recommended technique (Petersen 1995). Sound pressure level (SPL) is used as a metric to quantify the excitation to the piezoelectric disk. The voltage output of the piezoceramic disk is measured across a resistive shunt in parallel; the shunt impedance is varied from 100 Ohm to 1 M-Ohm. Time-domain data are measured using a National Instruments (NI) data acquisition system, and the NI LabVIEW software is used to record and process the data. The microphone signal is filtered using a Wavetek Hi/Lo Model 852 analog filter prior to signal acquisition. The high-pass filter cut-off is set to 1,000 Hz to eliminate line interference. The low-pass filter cut-off is set to 5,000 Hz for the conventional whistle, and is not used for the ultrasonic whistle.

In the post processing, first, the SPL and voltage output are compared. The frequencies with corresponding voltage and SPL peaks are identified in the frequency-domain; the SPL and voltage output are calculated at these frequencies.

Next, the root-mean-squared (RMS) values of the signals are calculated from the time-domain data. The voltage output is normalized with the measured SPL to a standard sound pressure level of 100 dB.

4.1 Conventional whistle

Two types of human-actuated conventional whistle experiments are conducted. The first experiment required the students to actuate the whistle at "average" effort; the second required actuation at "maximum" effort. The SPL-normalized voltage output and power density are shown in Fig. 5. The power density plot presents only the power for maximum actuation.

The maximum voltage generated is 0.33 V by Student 2. This student generated an average of 150 mV, or a factor of five to ten times, more voltage at the same SPL when compared to Student 1. The power output is calculated from voltage using $P = V^2/R$ where V is the voltage, and R is the shunt resistance. The power output at 100 dB is normalized by the piezoceramic disk volume to calculate the power density. The maximum power generated by

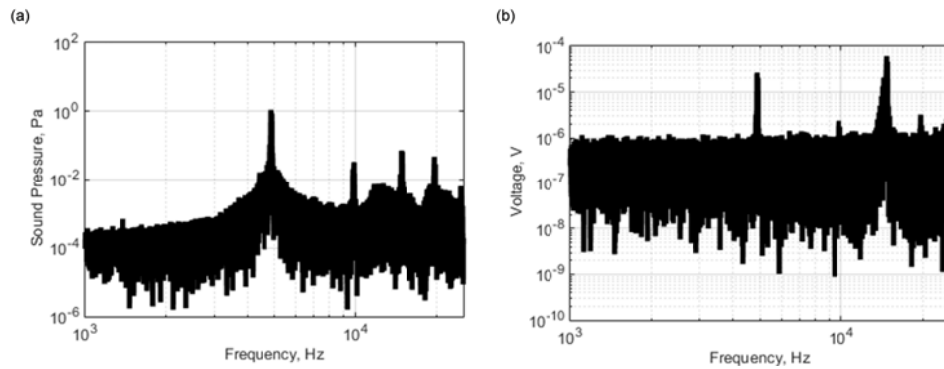


Fig. 7 Ultrasonic whistle undergoing human-actuation: (a) Sound pressure level and (b) voltage output as a function of frequency

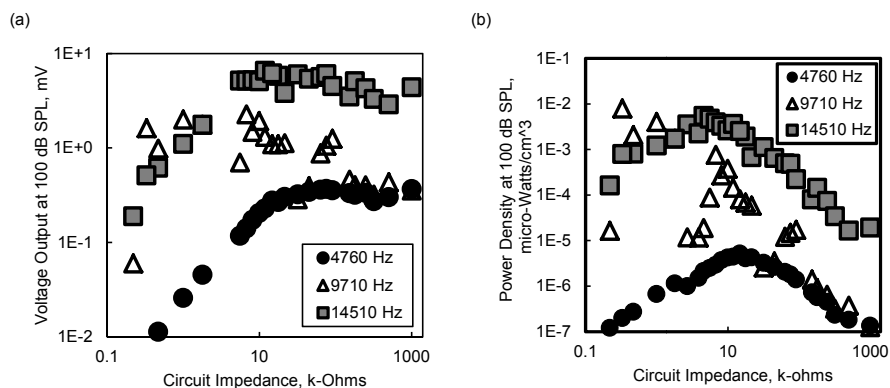


Fig. 8 Normalized voltage output and power density as a function of circuit impedance for the ultrasonic whistle undergoing human-actuation

Student 2 is $98.05 \mu\text{W}/\text{cm}^3$, which is $93.1 \mu\text{W}/\text{cm}^3$, or a factor of 11, greater than the power generated by Student 1. The difference in power output is attributed to differences in respiratory ability.

In a separate experiment, the conventional whistle is actuated using a pressure-regulated air supply; the supplied air is varied between 30 and 60 psi in 10 psi increments. The normalized voltage output and power density at each supply pressure are presented in Fig. 6.

The convergence of the normalized voltage output to a single curve indicates that sound pressure level is an accurate representation of the input to the whistle. The maximum voltage output is 35 mV. The maximum power generated is $2.15 \mu\text{W}/\text{cm}^3$. Some of the data above or below the curve are influenced by variation in other experimental variables and are considered as outliers; however, there is a repeating double-peak behavior. (This behavior is easier to observe in the experiments presented later.) The well-known reason for this behavior is the existence of multiple modes of vibration at different frequencies. As there are multiple resonance frequencies, there are also multiple corresponding “optimum” impedance values. It can be speculated that the first and second axisymmetric bending modes are being excited resulting in the observed double-peak response.

It is also noted that all power density plots are normalized to a 100 dB SPL and with the volume of the piezoceramic disk. The difference between human-actuation and actuation by pressure-regulated air indicates significant non-uniformity in human-actuation. Despite this non-uniformity, human-actuation consistently generated more power than actuation by pressure-regulated air for the tested supply pressure levels.

4.2 Ultrasonic whistle

The ultrasonic whistle is tested and the data are analyzed in the same manner as the conventional whistle. The ultrasonic whistle has a range of acoustic resonance frequencies, as shown in Fig. 7(a). The voltage output response shows similar behavior as shown in Fig. 7(b).

The frequencies at which the resonance behavior matches between both SPL and voltage output are 4,760 Hz, 9,710 Hz, and 14,510 Hz. The normalized voltage output and power density as a function of frequency and circuit impedance are shown in Fig. 8. The SPL and voltage output results are presented only for frequencies at which the sound pressure and voltage frequencies exhibit coherent behavior.

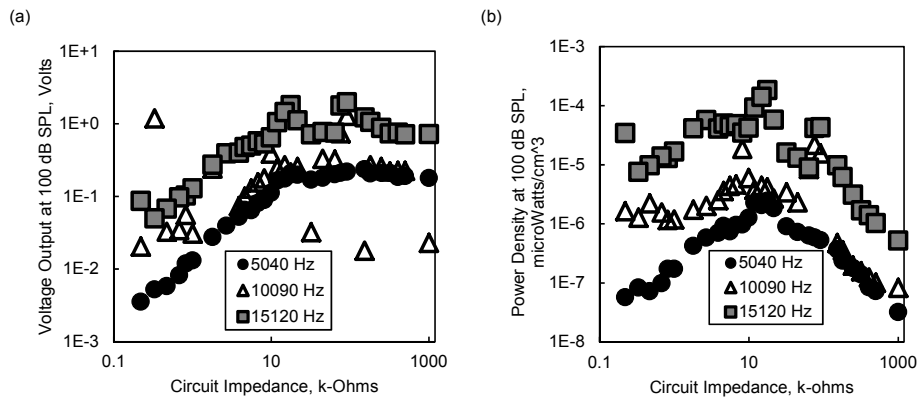


Fig. 9 Normalized voltage output and power density as a function of circuit impedance of an ultrasonic whistle in response to actuation using a pressure-regulated air supply

The maximum voltage output at 4,760 Hz is 0.37 mV, the maximum voltage output at 9,710 Hz is 2.27 mV, and the maximum voltage output at 14,510 Hz is 6.56 mV. The voltage output at 14,510 Hz is 18 times higher than the voltage output at 4,760 Hz and three times higher than the voltage output at 9,710 Hz. The maximum power output at 4,760 Hz is $5.2 \times 10^{-6} \mu W/cm^3$, the maximum power output at 9,710 Hz is $7.9 \times 10^{-3} \mu W/cm^3$, and the maximum power output at 14,510 Hz is $5.5 \times 10^{-3} \mu W/cm^3$. The power output at 9,710 Hz does show the double-peak response with respect to circuit impedance. It is anticipated that there are various modes of vibrations corresponding to the optimum resistances identified in Fig. 8(b). It is noted that the maximum power output at 14,510 Hz is three orders of magnitude higher than the maximum power output at 4,760 Hz.

In a separate experiment, the ultrasonic whistle is actuated using a pressure-regulated air supply in a similar manner as the conventional whistle. A single supply pressure of 1 psi is evaluated. The three frequencies where the acoustic response and the voltage output match are 5,040 Hz, 10,090 Hz, and 15,120 Hz. The normalized voltage output and power density at each of these frequencies are presented as a function of the circuit impedance in Fig. 9.

The maximum voltage output at 5,040 Hz is 0.24 mV, the maximum voltage output at 10,090 Hz is 1.29 mV, and the maximum voltage output at 15,120 Hz is 1.98 mV. The voltage output at 15,120 Hz is higher than the voltage output at 5,040 Hz by a factor of eight and higher than the voltage output at 10,090 Hz by a factor of 1.5. Both the 10 kHz and 15 kHz modes exhibit the dual-peak behavior, explained previously, as observed in the human-actuation tests for the 10 kHz mode. The maximum power output at 5,040 Hz is $2.4 \times 10^{-6} \mu W/cm^3$, the maximum power output at 10,090 Hz is $5.3 \times 10^{-5} \mu W/cm^3$, and the maximum power output at 15,120 Hz is $1.8 \times 10^{-4} \mu W/cm^3$. The power density at 15,120 Hz is a factor of 75 higher than the power density at 5,040 Hz, and a factor of three higher than the power density at 10,090 Hz. The higher power observed at high frequency modes is due to the increase in overall charge.

4.3 Comparison of whistles

The power density normalization facilitates comparison between conventional and ultrasonic whistles, and comparison to results published by other researchers. The power density at 100 dB SPL for each test configuration is given in Table 3.

The power output of a single piezoceramic disk mounted on the side of a conventional whistle is four orders of magnitude greater than the power generated by the same piezoceramic disk mounted at the end of an ultrasonic whistle. It is clear that the difference in power output is due to the difference in strain induced by the conventional whistle in comparison to the strain induced by the ultrasonic whistle. It is noted that the proof-mass used in the ultrasonic whistle was not optimized to match a particular frequency; hence it is expected that optimization will increase power output and this is the subject of future research.

The power generated by the two whistle prototypes is compared to power generated by two different resonators, as discussed in the literature review. The papers were chosen as the examples with the most power generated at experimental conditions that closely matched the current experiments. The conventional whistle generated similar voltage and power output as the referenced Helmholtz resonator. However, the ultrasonic whistle generated less power than the referenced pipe resonator. The lower power is attributable to the referenced paper discussing a multi-harvester system while the current research only contained a single harvester.

4.4 Discussion

Overall, human-actuation generates more power when compared to regulated air supply for the pressures tested here in both conventional and ultrasonic whistles. This unique response to human-actuation may be due to a unique acoustic coupling between lungs, mouth and the whistle chamber, which is the subject of future research.

Table 3 Comparison of power density at 100 dB SPL as a function of whistle type in response to human-actuation and pressure-regulated air supply

Test Configuration		Actuation Pressure (kPa)	Maximum V_{out} (at 100 dB SPL) (mV)	Power Density (at 100 dB SPL) ($\mu W/cm^3$)
Human-Actuation	Conventional	N/A	326	98.1 ($R = 18 k\Omega$)
	Ultrasonic	N/A	6.55	$5.47 \cdot 10^{-3}$ ($R = 4.6 k\Omega$)
Pressure-Regulated Air	Conventional	414	35	2.15 ($R = 22 k\Omega$)
	Ultrasonic	6.9	1.98	$1.83 \cdot 10^{-4}$ ($R = 18 k\Omega$)
Khan and Izhar (2013)	Helmholtz	N/A	315 (120 dB)	191 (120 dB) ($R = 66 \Omega$)
Li <i>et al.</i> (2012)	Pipe	$9 \cdot 10^{-3}$	1480 (110 dB)	55 (110 dB)

From a practical standpoint, the ultrasonic whistle appears to be much easier to actuate than the conventional whistle. It required less experimenter effort per two-second acquisition period, and the experimenter was less out of breath when compared to the actuation of the conventional whistle. This qualitative observation is also supported by the difference in supply pressures required to actuate the conventional whistle (greater than 20 psi) and the ultrasonic whistle (less than 1 psi).

5. Conclusions

This paper introduced the use of a whistle as a vibration energy source for powering low-power electronics such as a radio transmitter. Piezoelectric vibration energy harvesting using acoustic resonance is demonstrated in two types of whistles. Both human-actuation and pressure-regulated air actuation are examined. The conventional whistle generated four orders of magnitude more power compared to the ultrasonic whistle when normalized power is compared at a constant SPL. Human-actuation of the whistles consistently produced more power compared to actuation by a pressure-regulated air supply.

Acknowledgments

Authors would like to acknowledge the experimental contributions of Jacqui Devore, Tony Crawford, Joshua Harden, Thomas Super, Charles Wilson, and Bryce Horne who participated in the Smart Systems Summer Camp (S3C) during the summers of 2014 and 2015. The authors also acknowledge the support of the Old Dominion University Equipment Trust Fund and the Frank Batten College of Engineering and Technology. The authors acknowledge the support of the DataPhysics Corporation in providing the SignalCalc software.

References

- Aladwani, A., Aldraihem, O. and Baz, A. (2015), "Piezoelectric vibration energy harvesting from a two-dimensional coupled acoustic-structure system with a dynamic magnifier", *J. Vib. Acoust.*, 137.
- Anton, S.R. and Sodano, H.A. (2007), "A review of power harvesting using piezoelectric materials (2003-2006)", *Smart Mater. Struct.*, **16**, 1-21.
- Bibo, A., Li, G. and Daqaq, M.F. (2012), "Performance analysis of a harmonic-type aeroelastic micropower generator", *J. Intel. Mat. Syst. Str.*, 1045389X12438625.
- Bueche, F. (1969), *Introduction to physics for scientists and engineers*, New York, McGraw-Hill.
- Cook-Chennault, K.A., Thambi, N. and Sastry, A.M. (2008), "Powering MEMS portable devices—a review of non-regenerative and regenerative power supply systems with special emphasis on piezoelectric energy harvesting systems", *Smart Mater. Struct.*, **17**, 043001.
- Hattery, R. (2015), "Lumped parameter modeling and experimental evaluation of piezocomposite energy harvesters", *Mech. Aerosp. Eng.*, Norfolk, VA: Old Dominion University.
- Horowitz, S.B., Sheplak, M., Cattafesta III, L.N., et al. (2006), "A MEMS acoustic energy harvester", *J. Micromech. Microeng.*, **16**, 174.
- Horowitz, S.B., Sheplak, M., Cattafesta, L.N. and Nishida, T. (2005), "MEMS acoustic energy harvester", *PowerMEMS 2005*. Tokyo, Japan, 4.
- Karami, M.A. and Inman, D.J. (2012), "Powering pacemakers from heartbeat vibrations using linear and nonlinear energy harvesters", *Appl. Phys. Lett.*, 100.
- Khan F.U. and Izhar, E. (2013), "Acoustic-based electrodynamic energy harvester for wireless sensor nodes application", *Int. J. Mater. Sci. Eng.*, **1**, 7.
- Kim, S.H., Ji, C.H., Galle, P., et al. (2009), "An electromagnetic energy scavenger from direct airflow", *J. Micromech. Microeng.*, **19**, 094010.
- Leissa, A.W. (1969), *Vibration of plates*, Washington, Scientific and Technical Information Division, National Aeronautics and Space Administration; for sale by the Supt. of Docs.
- Li, B., Ho You, J. and Kim, Y.J. (2013), "Low frequency acoustic energy harvesting using PZT piezoelectric plates in a straight tube resonator", *Smart Mater. Struct.*, **22**, 9.
- Li, B., Ho You, J., Laviage, A.J. and Kim, Y.J. (2012), "Acoustic energy harvesting using quarter-wavelength straight-tube resonator", *Proceedings of the ASME 2012 International*

- Mechanical Engineering Congress & Exposition*. Houston, Texas, USA.
- Liu, F., Phipps, A., Horowitz, S., et al. (2008), "Acoustic energy harvesting using an electromechanical Helmholtz resonator", *J. Acoust. Soc. Am.*, **123**, 1983-1990.
- Matsuda, T., Tomii, K., Hagiwara, S., et al. (2013), "Helmholtz resonator for Lead Zirconate Titanate acoustic energy harvester", *J. Phys.: Conference Series*. IOP Publishing, 012003.
- Moriyama, H., Tsuchiya, H. and Oshino, Y. (2013), "Energy harvesting with piezoelectric element using vibroacoustic coupling phenomenon", *Adv. Acoust. Vib.*
- Paradiso, J.A. and Starner, T. (2005), "Energy scavenging for mobile and wireless electronics", *Ieee Pervasive Computing*, **4**, 18-27.
- Petersen, E.C. (1995), Application Note: An Overview of Standards for Sound Power Determination. Denmark, 12.
- Piezo Systems I. (2015), *PSI-5A4E Single Layer Disks*. Available at: <http://www.piezo.com/prodsheet3disk5A.html>.
- Pillai, M.A. and Deenadayalan, E. (2014), "A review of acoustic energy harvesting", *Int. J. Precision Eng. Manufact.*, **15**, 949-965.
- Priya, S. and Inman, D.J. (2009), *Energy harvesting technologies*, New York: Springer.
- Reddy, J.N. (1999), *Theory and analysis of elastic plates*, Philadelphia, PA: Taylor & Francis.
- Shames, I.H. and Dym, C.L. (1985), *Energy and finite element methods in structural mechanics*, Washington, New York: Hemisphere Pub. Corp.; McGraw-Hill.
- Sherrit, S. (2008), "The physical acoustics of energy harvesting. *Proceedings of the IEEE International Ultrasonics Symposium*, Beijing, China.
- Sodano, H., Inman, D. and Park, G. (2004), "A review of power harvesting from vibration using piezoelectric materials", *Shock Vib. Digest*, **36**, 197-205.
- Starner, T. and Paradiso, J.A. (2004), *Human generated power for mobile electronics*, CRC Press, 1-35.
- Sue, C.Y. and Tsai, N.C. (2012), "Human powered MEMS-based energy harvest devices", *Appl. Energy*, **93**, 390-403.
- Sun, C.L., Mu, X.J., Siow, L.Y., et al. (2014), "A miniaturization strategy for harvesting vibration energy utilizing helmholtz resonance and vortex shedding effect", *IEEE Electron Device Lett.*, **35**, 675-675.
- Szilar, R. (1973), *Theory and analysis of plates: classical and numerical methods*, Englewood Cliffs, N.J.: Prentice-Hall.
- Wang, W.C., Wu, L.Y., Chen, L.W. and Liu, C.M. (2010), "Acoustic energy harvesting by piezoelectric curved beams in the cavity of a sonic crystal", *Smart Mater. Struct.*, **19**, 7.
- Wu, L.Y., Chen, L.W. and Liu, C.M. (2009), "Acoustic energy harvesting using resonant cavity of a sonic crystal", *Appl. Phys. Lett.*, **95**, 3.
- Yang, A., Li, P., Wen, Y., et al. (2014), "Note: High-efficiency broadband acoustic energy harvesting using Helmholtz resonator and dual piezoelectric cantilever beams", *Rev. Sci. Instrum.*, **85**, 066103.